

AQUARIUS' COMBINED ACTIVE PASSIVE ALGORITHM FOR OCEAN SURFACE SALINITY AND WIND RETRIEVAL

Wenqing Tang, Simon Yueh, Alexander Fore, and Akiko Hayashi
Jet Propulsion Laboratory, California Institute of Technology, Pasadena, CA, USA

1. INTRODUCTION

Aquarius' combined passive/active L-band microwave instrument has been in operation since 25 August 2011, mapping the ocean surface salinity field from space [1]. The measurement principle is based on the response of the L-band (1.413 GHz) sea surface brightness temperatures to sea surface salinity, with primary objective to monitor the seasonal and interannual variation of the large-scale features of the surface salinity field in the open ocean with a spatial resolution of 150 km and a retrieval accuracy of 0.2 psu globally on a monthly basis.

This paper describes the updated Combined Active-Passive (CAP) retrieval algorithm, which uses Aquarius' brightness temperature and radar backscatter from sea surfaces for simultaneous retrieval of surface salinity and wind. Unlike the algorithm developed by the Remote Sensing System (RSS), the Jet Propulsion Laboratory (JPL) CAP algorithm does not require monthly SSS maps to constrain the salinity retrieval. Furthermore the RSS algorithm fully uses the National Center for Environmental Predictions (NCEP) wind for data correction, while the CAP algorithm uses the NCEP wind only as a loose constraint. The major updates to the CAP algorithm include the galactic reflection correction, Faraday rotation and antenna pattern correction as well as the geophysical model functions (GMF) of wind, wave and rain impacts. Recognizing the limitation of geometric optics scattering, we improve the modeling of the reflection of galactic radiation; the results are improved salinity accuracy and significantly reduced ascending-descending bias in the salinity retrievals. We also describe the updated performance assessment of the scatterometer-only and CAP wind speed products with more than 2 years of data.

2. AQUARIUS GEOPHYSICAL MODEL FUNCTION

As described in Yueh et al. [2], the Aquarius radar backscatter σ_0 and radiometer excess emissivity $\Delta\epsilon$ are modeled as functions of surface wind speed (w) and relative azimuth angle (ϕ) using rain-free data. In addition to the surface wind, we found that σ_0 and $\Delta\epsilon$ at L-band are also under the influence of the ocean waves [3] and surface rain [4]. Our analysis of the wave impact included the National Oceanic and Atmospheric Administration (NOAA) WaveWatch-3 (WW3) Significant Wave Height (SWH) in the matchup data set. The Aquarius data were binned as a function of the SWH at 1-m step, as well as wind speed and direction. The directional dependence of the Aquarius data at each wind speed and SWH was analyzed, and it was concluded that the influence of the SWH on the wind direction dependence is small, about 10 percent of the

directional amplitude. For each Aquarius antenna beam, we represent the Aquarius GMF by the following cosine series to model the impact of wind and waves on L-band radar backscatter and brightness temperatures:

$$\sigma_{0,p}(w, \phi, SWH) = A_{0,p}(w, SWH)[1 + A_{1,p}(w)\cos\phi + A_{2,p}(w)\cos2\phi] \quad (1)$$

$$\Delta e_p(w, \phi, SWH) = e_{0,p}(w, SWH) + e_{1,p}(w)\cos\phi + e_{2,p}(w)\cos2\phi \quad (2)$$

where the subscript ‘‘p’’ indicates the polarization, which can be VV or HH for radar backscatter (σ_0) and V or H for radiometer excess surface emissivity (Δe). Given the GMF for excess surface emissivity, we use the following functional form for the radiometer model function, which relates the brightness temperatures to SSS, SST (T_s), SWH, w and ϕ :

$$T_{Bp}(SSS, T_s, w, \phi, SWH, \theta) = T_{Bpflat}(SSS, T_s, \theta) + T_s \Delta e_p(w, \phi, SWH) \quad (3)$$

We have derived the $A_{n,p}$ and $e_{n,p}$ coefficients from the rain-free data acquired from 25 August 2011 to 30 June 2013.

Tang et al. [4] examined, under rainy conditions (as predicted by the collocated SSMI/S rain rates), the L-band residual signals, i.e. the difference between Aquarius measurements and the model predictions calculated from Eq. (1) & (2). They found the presence of rain increases the radar backscatter and surface emissivity at low wind speeds, but the effects decrease with increasing wind speed. It seems that raindrops cause the most excitation on a calm water surface, resulting in extra roughness when in low winds; while at high winds, the wind-generated roughness dominates. They also show that the azimuthal directional dependence of L-band signals under rainy conditions are small for low wind, while agree well with the rain free model (A_1 & A_2 for radar and e_1 & e_2 for radiometer). Based on these results, therefore, we introduce δA_0 and δe_0 as the rain-induced surface roughness correction on radar and radiometer GMF respectively, modify Eq. (1) and (2) as,

$$\sigma_{0,p}(w, \phi, SWH, R) = [A_{0,p}(w, SWH) + \delta A_{0,p}(w, R)][1 + A_{1,p}(w)\cos\phi + A_{2,p}(w)\cos2\phi] \quad (4)$$

$$\Delta e_p(w, \phi, SWH, R) = e_{0,p}(w, SWH) + \delta e_{0,p}(w, R) + e_{1,p}(w)\cos\phi + e_{2,p}(w)\cos2\phi \quad (5)$$

where R is the surface rain rate. No rain correction is implemented for wind speed exceeds 12 m s^{-1} and 17 m s^{-1} for radar and radiometer, respectively, due to lack of enough sampling.

3. SSS RETRIEVAL WITH CAP ALGORITHM

The CAP algorithm retrieves the salinity and wind simultaneously by finding the best-fit solution to minimize the difference between the Aquarius data and model functions [5]. The cost function for the CAP Version 3 algorithm is

$$C_{ap}(w, \phi, SSS) = \sum_{p=V,H} \frac{(T_{BP} - T_{BPM})^2}{\Delta T^2} + \sum_{p=VV,HH} \frac{(\sigma_{0P} - \sigma_{0PM})^2}{(\gamma_p \sigma_{0p})^2} + \frac{(w - w_{NCEP})^2}{\Delta w^2} + \frac{\sin^2(\frac{\phi - \phi_{NCEP}}{2})}{\delta^2} \quad (6)$$

The weighting factors for the Aquarius data are set according to the expected measurement and modeling uncertainties. We let ΔT be the Noise-Equivalent-Delta-T (NEDT) of radiometer and γ_p be 1.4 times of the radar measurement sensitivity (k_{pc}). The values of NEDT and k_{pc} , a function of signal-to-noise ratio, have been pre-computed and saved in the Aquarius L2 data files. The value of Δw is 1.5, a rather weak constraint because the accuracy of CAP wind speed is estimated to be about 0.7 ms^{-1} [2]. The value of δ is 0.2, which will constrain the wind direction to be within an RMS deviation of 11 degrees from the NCEP wind direction.

We assess the accuracy of Aquarius CAP wind by performing comparison with the SSMI/S wind and triple collocation analysis. The triple collocation analysis using the SSMI/S, CAP and ECMWF winds indicates that the accuracy of CAP wind speed is about 0.7 m/s, essentially the same as that of SSMI/S wind speed and less than the 0.9 m/s error for the ECMWF.

The accuracy of CAP salinity is assessed by comparison with ARGO's monthly gridded salinity products obtained from the Asia-Pacific Data-Research Center (APDRC) and Japan Agency For Marine-Earth Science And Technology (JAMSTEC). Averaged between 40°S and 40°N globally, the RMS difference (Fig. 1) of CAP retrieved SSS with (CAP_RC) or without (CAP) rain correction performs better than the RSS V2.5.1 SSS (L2) consistently on monthly basis. The effect of rain correction on SSS retrieval, quantified as ΔSSS (i.e., CAP_RC - CAP), is estimated causing about 20% difference on the annual amplitude of the mixed layer salt storage tendency.

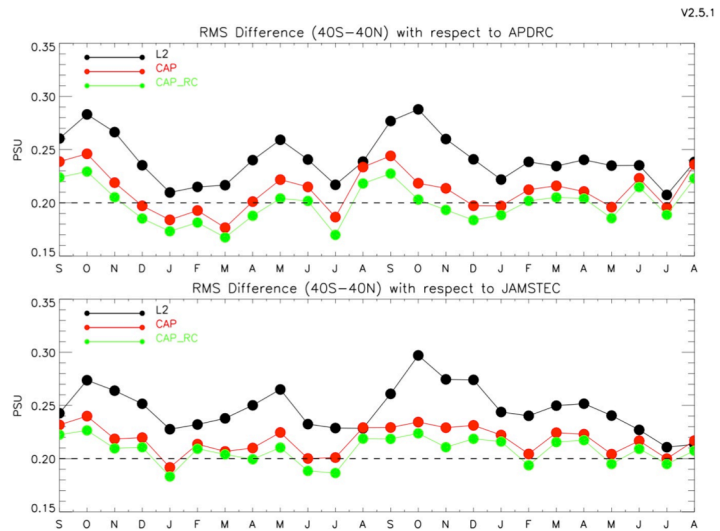


Figure 1. The RMS difference between monthly-averaged Aquarius SSS (L2, CAP and CAP_RC) with respect to APDRC (top) and JAMSTEC-ARGO (bottom) monthly gridded products.

Aquarius SSS are also validated with the salinity measurements from the global tropical moored buoy arrays, which includes the TAO/TRITON array in the Pacific, the PIRATA array in the Atlantic, and RAMA in the Indian Ocean. Although all three Aquarius derived SSS show comparable correlation with buoy measurements (7-days moving averaged daily), the standard deviation of CAP and CAP_RC are smaller than L2, while CAP_RC has the smallest bias.

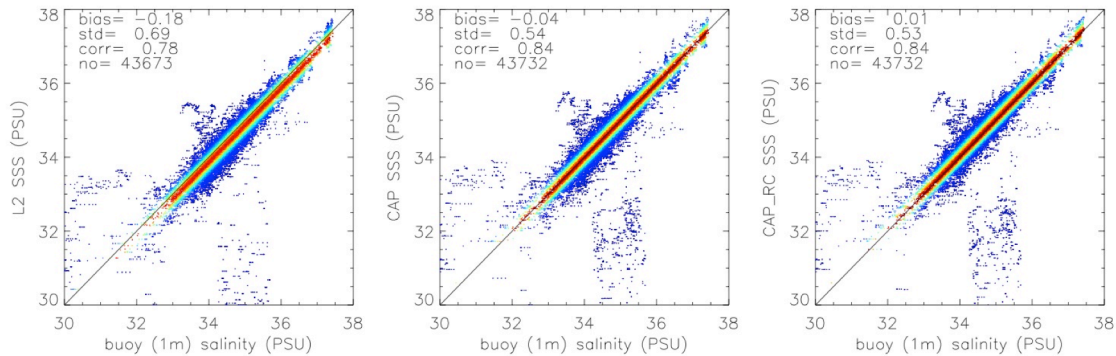


Figure 2. Scatter plots of the Aquarius retrieved SSS (from left to right): L2, CAP, and CAP_RC vs. buoy salinity measured at 1m, created from daily time series with 7-days moving averages from Sep.1 2011 to Aug. 31, 2013, collocated at moored buoy array locations.

4. ACKNOWLEDGMENT

The work described in this paper was carried out by the Jet Propulsion Laboratory, California Institute of Technology under a contract with the National Aeronautics and Space Administration.

5. REFERENCES

- [1] Lagerloef, G., Colomb Fr, Le Vine D, et al. (2008), The Aquarius/Sac-D Mission: Designed To Meet The Salinity Remote-Sensing Challenge, *Oceanography*, Vol. 21, Pages: 68-81.
- [2] Yueh, S. H., W. Tang, A. Fore, G. Neumann, A. Hayashi, A. Freedman, J. Chaubell, and G. Lagerloef (2013), L-band Passive and Active Microwave Geophysical Model Functions of Ocean Surface Winds and Applications to Aquarius Retrieval. *IEEE TGRS*, 51, 4619-4632.
- [3] Yueh, S., W. Tang, A. Fore, and A. Hayashi (2014), Impact of Ocean Waves on L-band Passive and Active Microwave Observation of Sea Surfaces, Submitted to *IEEE TGRS*.
- [4] Tang, W., S. H. Yueh, A. Fore, G. Neumann, A. Hayashi, and G. Lagerloef (2013), The rain effect on Aquarius' L-band sea surface brightness temperature and radar backscatter, *Remote Sensing of Environment*, 137, 147-157.
- [5] Yueh, S. H. and M. J. Chaubell (2012), Sea Surface Salinity and Wind Retrieval Using Combined Passive and Active L-Band Microwave Observations, *IEEE Trans. Geoscience and Remote Sensing*.